THE JOURNAL OF BIOLOGICAL CHEMISTRY VOL. 290, NO. 37, pp. 22520–22531, September 11, 2015

CUX2 Protein Functions as an Accessory Factor in the Repair of Oxidative DNA Damage*

Received for publication, March 9, 2015, and in revised form, July 27, 2015 Published, JBC Papers in Press, July 28, 2015, DOI 10.1074/jbc.M115.651042

Ranjana Pal[‡1,2], Zubaidah M. Ramdzan[‡1,3], Simran Kaur[‡§], Philippe M. Duquette[¶4], Richard Marcotte[‖], Lam Leduy[‡], Sayeh Davoudi[§5], Nathalie Lamarche-Vane[¶], Angelo Iulianella[**], and Alain Nepveu[‡§‡‡§§6]

*From the [‡]Goodman Cancer Research Centre and Departments of [§]Biochemistry, [‡‡]Medicine, [§§]Oncology, and [¶]Anatomy and Cell Biology, McGill University, Montreal, Quebec H3A 1A3, Canada, [‖]Princess Margaret Cancer Centre, University Health Network, Toronto M5G 1L7, Canada, and **Department of Medical Neuroscience, Dalhousie University, Life Science Research Institute, Halifax B3H 4R2, Canada*

Background: CUX2 contains three Cut repeat domains and is expressed in postmitotic neurons.
Results: Cut repeats stimulate the OGG1 DNA glycosylase, and lower or higher CUX2 expression, respectively, delays or accelerates repair of oxidative DNA damage.
Conclusion: CUX2 functions as an accessory factor in base excision repair.
Significance: CUX2 contributes to the maintenance of genome integrity in long lived neurons.

CUX1 and CUX2 proteins are characterized by the presence of three highly similar regions called Cut repeats 1, 2, and 3. Although CUX1 is ubiquitously expressed, CUX2 plays an important role in the specification of neuronal cells and continues to be expressed in postmitotic neurons. Cut repeats from the CUX1 protein were recently shown to stimulate 8-oxoguanine DNA glycosylase 1 (OGG1), an enzyme that removes oxidized purines from DNA and introduces a single strand break through its apurinic/apyrimidinic lyase activity to initiate base excision repair. Here, we investigated whether CUX2 plays a similar role in the repair of oxidative DNA damage. *Cux2* knockdown in embryonic cortical neurons increased levels of oxidative DNA damage. *In vitro*, Cut repeats from CUX2 increased the binding of OGG1 to 7,8-dihydro-8-oxoguanine-containing DNA and stimulated both the glycosylase and apurinic/apyrimidinic lyase activities of OGG1. Genetic inactivation in mouse embryo fibroblasts or *CUX2* knockdown in HCC38 cells delayed DNA repair and increased DNA damage. Conversely, ectopic expression of Cut repeats from CUX2 accelerated DNA repair and reduced levels of oxidative DNA damage. These results demonstrate that CUX2 functions as an accessory factor that stimulates the repair of oxidative DNA damage. Neurons produce a high level of reactive oxygen species because of their dependence on aerobic oxidation of glucose as their source of energy. Our results suggest that the persistent expression of CUX2 in postmitotic neurons contributes to the maintenance of genome integrity through its stimulation of oxidative DNA damage repair.

Reactive oxygen species (ROS)[7] generated through cellular metabolism represent a major threat to the integrity of DNA. Base excision repair (BER) is the major pathway for the repair of oxidative DNA damage (1). It has been known for some time that oxidative DNA damage accumulates in the mammalian brain with aging (2–6). This accumulation is considered a possible cause for the progressive loss of neurons associated with aging and therefore potentially associates BER deficiency with age-related neurodegeneration (7). Indeed, experimental evidence indicates that defective BER processing can promote postmitotic neuronal cell death and neurodegenerative disease (8–10). In particular, defective base excision repair was demonstrated in brain from individuals with Alzheimer disease and amnestic mild cognitive impairment (11).

In mammalian cells, four DNA glycosylases specific for oxidized bases have been identified: 8-oxoguanine DNA glycosylase 1 (OGG1), Nth homolog 1 (NTH1), and Nei-like 1 and 2 (NEIL1 and NEIL2). Although each of these glycosylases exhibits substrate preference, none has absolute specificity (for a review, see Ref. 12). Among the most abundant of ROS-induced adducts in DNA is 7,8-dihydro-8-oxoguanine (8-oxoG). This altered base can mispair with adenine and cause G-C to T-A transversion mutations (13). 8-oxoG is removed by OGG1 or NEIL1 depending on DNA structure (14–17). DNA glycosylases for oxidized bases perform two enzymatic activities. The glycosylase activity involves hydrolysis of the *N*-glycosidic bond to generate an apurinic/apyrimidinic (AP) site. Subsequently, an AP lyase activity generates a single strand nick 3′ to the AP

* This work was supported in part by Canadian Institutes of Health Research Grant MOP-326694 (to A. N.). The authors declare that they have no conflicts of interest with the contents of this article.
[1] Both authors contributed equally to this work.
[2] Supported by a studentship from the McGill Integrated Cancer Research Training Program. Present address: Dept. of Biological Sciences, Presidency University, Kolkata, India 700073.
[3] Supported by a fellowship from the Fonds de la recherche en santé du Québec (FRSQ).
[4] Supported by a doctoral studentship from the FRSQ.
[5] Supported by a studentship from the Cole Foundation.
[6] To whom correspondence should be addressed: Goodman Cancer Research Centre, 1160 Pine Ave. West, Rm. 414, Montreal, Quebec H3A 1A3, Canada. Tel.: 514-398-5839; Fax: 514-398-6769; E-mail: alain.nepveu@mcgill.ca.

[7] The abbreviations used are: ROS, reactive oxygen species; BER, base excision repair; 8-oxoG, 7,8-dihydro-8-oxoguanine; AP, apurinic/apyrimidinic; CR, Cut repeat; MEF, mouse embryo fibroblast; HD, homeodomain; NLS, nuclear localization signal; 7-AAD, 7-aminoactinomycin D; OGG1, 8-oxoguanine DNA glycosylase 1; NTH1, Nth homolog 1; NEIL, Nei-like; HOXB3, homeodomain protein B3; hOGG1, human OGG1.

site via β (OGG1 and NTH1) or β-δ (NEIL1 and NEIL2) elimination. End processing of the resulting single strand break is then performed by APE1 or polynucleotide kinase 3′-phosphatase, and repair synthesis and ligation are accomplished by the short patch or long patch pathways (18, 19).

BER is essential to all organisms, and DNA glycosylases, the key enzyme in this pathway, are highly conserved in evolution. Research on DNA glycosylases was originally carried out in bacterial systems, mostly *Escherichia coli*, and enzymes with similar activities were rapidly identified in eukaryotes and mammals (20, 21). Further research has led to the identification of a number of proteins that modulate the activity of BER enzymes through various mechanisms. XRCC1, a scaffold protein that modulates both the early and late steps of BER, was found to interact with many glycosylases, including OGG1, and stimulate their glycosylase activity (22–25). APE1 was shown to stimulate the glycosylase activity of OGG1 by displacing it from the resulting abasic site and therefore enabling a more rapid recycling of OGG1 (26, 27). NEIL1 was reported also to stimulate OGG1 via a similar mechanism (28). YB-1, an RNA- and DNA-binding protein with multiple roles in transcription and RNA regulation, was found to interact with many BER proteins and stimulate the enzymatic activities of NTH1 and NEIL2 (29, 30). HMGB1, a protein with DNA bending capacity, stimulates the activities of the APE1 and FEN1 endonucleases and interacts with several BER enzymes (31). GADD45 promotes the interaction between a 5′-methylcytosine deaminase and the thymine-DNA glycosylase and increases the removal of 5-formylcytosine and 5-carboxylcytosine, a process that has been implicated in DNA demethylation (32, 33). Both OGG1 and NEIL1 were shown to bind to PARP-1 and stimulate its poly-(ADP-ribosyl)ation activity, thereby promoting the recruitment of downstream BER effectors such as XRCC1. In turn, PARP-1 inhibits the enzymatic activity of these DNA glycosylases (34, 35). Globally, the above cited studies indicate that several proteins can participate in BER complex formation and modulate the enzymatic activities of distinct BER enzymes.

In *Drosophila*, *cut* was shown to specify cell type identity in the sensory organs (36, 37). Subsequent work in *Drosophila* implicated *cut* in the regulation of dendrite branching pattern (38–41). A similar function in the brain of mammals has now been established for the orthologs of *cut* (42–45). There are two *Cut* homeobox genes in mammals, *Cux1* and *Cux2*, that fulfill additive and complementary roles in the stimulation of dendrite branching, spine development, and synapse formation in layer II-III neurons of the cerebral cortex (43, 45, 46). CUX1 and CUX2 proteins are characterized by the presence of a Cut-type homeodomain and three highly similar regions of ~70 amino acids called Cut repeats 1, 2, and 3 (CR1, CR2, and CR3) (47–49). Cut repeats were originally characterized as domains that bind to DNA in cooperation with one another or with the Cut homeodomain (50, 51). More recently, Cut repeats of CUX1 were shown to bind to OGG1 and stimulate both its glycosylase and AP lyase enzymatic activities (52, 53). Knockdown or genetic inactivation of CUX1 was found to delay the repair of oxidative DNA damage, whereas higher CUX1 expression accelerated DNA repair. These findings suggest that a physiological role of CUX1 is to protect cells against mutagenesis in situations of oxidative stress. In cancer, however, this biochemical activity is exploited by RAS-driven tumor cells that generate high levels of ROS. Indeed, higher CUX1 expression prevents RAS-induced senescence and promotes the development of tumors from cells that spontaneously acquire an activating *Kras* mutation (53). Conversely, CUX1 knockdown is synthetic lethal to KRAS-transformed cells (53, 54). Together, these findings illustrated a case of non-oncogene addiction whereby cancer cells have become acutely dependent on the heightened expression and activity of a protein that is not itself an oncogene (55, 56).

Whereas CUX1 is expressed in virtually all mouse tissues, CUX2 exhibits a more restricted pattern of expression (49, 57, 58). In the liver, CUX2 functions as a female-specific transcription factor (59, 60). In the nervous system, CUX2 is expressed in cortical neurons (43, 45), the hippocampus (61), the spinal cord (62, 63), dorsal root ganglions (64), and the olfactory epithelium (65). Both CUX1 and CUX2 proteins continue to be expressed in postmitotic neurons (66). Biochemical analysis of CUX2 revealed that various combinations of its DNA binding domains (CR1CR2, CR2CR3 and the homeodomain (CR2CR3HD), and CR3HD) exhibit DNA binding preferences similar to the corresponding domains of CUX1 (67). However, all CUX2 DNA binding domains exhibit very rapid DNA binding kinetics, suggesting that CUX2 does not bind stably to DNA, whereas an isoform of CUX1, called p110 CUX1, interacts stably with DNA and can function as a transcriptional activator or repressor depending on promoter context (for reviews, see Refs. 68 and 69). A proteolytically processed isoform of CUX2 that resembles p110 CUX1 has not been identified.

In the present study, we investigated whether CUX2, like CUX1, could function as an accessory factor in the repair of oxidative DNA damage. We first measured the effect of *Cux2* knockdown on oxidative DNA damage in embryonic cortical neurons and then analyzed the DNA repair capabilities of mouse embryo fibroblasts derived from a *Cux2* knock-out mouse. Our results show that genetic inactivation or knockdown of *Cux2* negatively affects the repair of oxidative DNA damage, whereas ectopic expression of various recombinant proteins that contain CUX2 Cut repeats can accelerate DNA repair. *In vitro*, Cut repeats from CUX2 can stimulate both the glycosylase and AP lyase activities of OGG1. Finally, we show that HCC38 breast tumor cells are acutely dependent for their survival on the DNA repair activities of CUX2, thereby revealing another case of non-oncogene addiction involving a CUX protein.

Experimental Procedures

Primary Cortical Neuron Culture—Cortical neurons from E17.5 rat embryos (Charles River) were dissociated mechanically and plated on 6-well plates treated with poly-D-lysine (0.1 mg/ml; Sigma-Aldrich) at a density of 5×10^6 cells/well. Neurons were cultured in a 3% O_2 incubator in DMEM containing 10% fetal bovine serum (FBS) overnight, and the medium was replaced by Neurobasal-A medium supplemented with 2% B27 and 1% L-glutamine (Invitrogen) (70).

Cell Culture and Virus Production—Primary mouse embryonic fibroblasts (MEFs) were grown at 37 °C in 5% CO_2 and 3% O_2, whereas HCC38 were grown at 37 °C in 5% CO_2 and atmospheric O_2. Lentiviruses expressing CUX2 fragments (CR1CR2, CR2CR3HD, CR3HD, and *lacZ*) and short hairpin RNA against rat *Cux2* (MISSION shRNA pLKO.1, Sigma) and human *CUX2* (The RNAi Consortium) were produced as described previously (53). Protein expression levels of endogenous CUX2 were determined using anti-CUX2-356 antibody (67), whereas recombinant CUX2 proteins were detected using anti-HA (MMS-101R, Covance).

Cell Proliferation Assay and Apoptosis Assay—8×10^2 HCC38 cells expressing shRNA against *CUX2* or luciferase were plated in five 96-well culture plates. A cell proliferation assay using WST-1 reagent (Roche Applied Science) was performed according to the manufacturer's instructions. Briefly, every 24 h, the medium in one 96-well plate was replaced with medium containing WST-1 reagent at 1:10 dilution, and cells were incubated with WST-1 reagent for 4 h before absorbance at 440 nm was measured on a Varioskan plate reader with the SkanIt software (Thermo Scientific). The experiment was repeated for the remaining four plates every 24 h. Cell proliferation was also measured over 4 days using the IncuCyte live cell imaging system (Essen Bioscience) housed in a 37 °C incubator at 5% CO_2. 5×10^4 cells were cultured in 6-well plates, and bright field images were acquired at 10× magnifications from six locations per well at 4-h intervals. To monitor apoptosis, HCC38 cells were harvested on day 2 after infection and double stained with annexin V conjugated to phycoerythrin and 7-aminoactinomycin (7-AAD) (Apoptosis Detection Kit-1, BD Biosciences). Apoptotic events were analyzed using FlowJo 887 software. All these experiments were repeated twice in triplicates.

Bacterial Protein Expression—Histidine-tagged CUX2 peptides CR1CR2, CR2CR3HD, and CR3HD and CUX1 CR1CR2 were expressed in the pET-15b vector as described previously (67, 71). Plasmids expressing histidine-tagged CUX2 CR1, CR2, and $CR1^{mut}$ were prepared by inserting gBlocks gene fragments (Integrated DNA Technologies) into pDEST14 according to the manufacturer's instructions (Invitrogen). $CR1^{mut}$ carries two point mutations replacing glutamic acids with alanine in the first helix of Cut repeat 1 at positions 557 and 564 of CUX2 (CUX2 accession number NP_056082). All CUX2 plasmid maps and sequences are available upon request. Histidine-tagged homeodomain protein B3 (HOXB3) was obtained from Addgene (72), and GST-tagged OGG1 was a generous gift from Drs. Nicole Noren Hooten and Michele Evans (35). All proteins were expressed in the BL21 strain of *E. coli* and were induced with isopropyl β-D-thiogalactopyranoside. His-tagged fusion proteins for the *in vitro* cleavage assay were bound to nickel beads (Qiagen) and eluted with 250 mM imidazole followed by several buffer exchanges carried out in 3-kDa molecular mass-cutoff dialysis membrane (Spectra/Pro Dialysis tubing, Spectrum Laboratories) to bring down the imidazole concentration to less than 0.1 μM. GST-tagged OGG1 was bound to glutathione-Sepharose beads (GE Healthcare) following the manufacturer's instructions. Purified GST-OGG1 proteins were used in the pulldown assays only, whereas OGG1 from New England Biolabs was used in the cleavage assays.

Single Cell Gel Electrophoresis—For H_2O_2 treatment, cells at ~80% confluence were treated with 10 μM H_2O_2 on ice for 20 min. After treatment, cells were allowed to recover at 37 °C in fresh medium for the indicated periods of time before harvesting. Comet assays were carried out using precoated slides according to the manufacturer's protocol (Trevigen). The slides were stained with propidium iodide and visualized with Axiovert 200M microscope with an LSM 510 laser module (Zeiss). Comet tail moments were measured on a minimum of 50 cells using CometScore software (TriTeck Corp.).

In Vitro Binding Assay—Bacterially expressed His-tagged CUX2 proteins as well as proteins from bacteria carrying the empty His tag vector were bound to cobalt Dynabeads magnetic beads (Life Technologies) and incubated overnight with 100 ng of purified GST-OGG1 proteins. Binding assays were also conducted with purified GST and GST-OGG1 bound to glutathione-Sepharose beads (GE Healthcare) and incubated overnight with 400 ng of eluted His-tagged CUX2 proteins. In both binding assays, the samples were washed five times with Nonidet P-40 buffer (50 mM Tris, pH 8.0, 150 mM NaCl, 50 mM NaF, and 1% Nonidet P-40 supplemented with protease inhibitor mixture (Roche Applied Science)) and separated by SDS-PAGE followed by immunoblotting with anti-OGG1 antibody (PA1-31402, Thermo Scientific) and anti-His antibody (H1029, Sigma).

Immunoprecipitation—293T cells were transfected with CUX2-HA or the empty vector in the presence of Lipofectamine 2000 (Invitrogen) according to the manufacturer's instructions. Cells were lysed by sonication in lysis buffer (20 mM Tris, pH 8.0, 150 mM NaCl, and 1% Nonidet P-40) supplemented with a protease inhibitor mixture and centrifuged at 13,000 × *g* for 10 min. Endogenous OGG1 proteins were immunoprecipitated with anti-OGG1 and protein A Dynabeads (Invitrogen). The samples were separated by SDS-PAGE followed by immunoblotting with anti-OGG1 antibody and anti-HA.

In Vitro 8-OxoG Cleavage Assay—Double-stranded 31-mer oligonucleotides containing an 8-oxoG at the 16th position (Midland) were labeled with [γ-^{32}P]ATP at the 5′-end of the top strand (*) using polynucleotide kinase and used in cleavage and DNA binding assays as described previously (82). Cleavage reactions with bacterially purified proteins were conducted using 50 nM hOGG1 (New England Biolabs, Ipswich, MA) and 50 nM BSA or the indicated proteins unless otherwise indicated in 25 mM NaCl, 10 mM Tris, pH 7.5, 1 mM $MgCl_2$, 5 mM EDTA, pH 8.0, 5% glycerol, 1 mM DTT, and 1 pmol of ^{32}P-radiolabeled double-stranded oligonucleotides containing an 8-oxoG base. Note that when using His-tagged fusion proteins it is important at the end of the purification to carry out several buffer exchanges to reduce the imidazole concentration. In our hands, OGG1 was stimulated by imidazole at concentrations above 0.4 mM. Cleavage reactions were performed at 37 °C as described previously (73). Briefly, reactions were performed for 30 min in 37 °C and stopped with 15 mM EDTA, 0.175% SDS, and 1 mg/ml proteinase K for 30 min as described previously (73). Formamide DNA loading buffer (90% formamide with 0.05% bromphe-

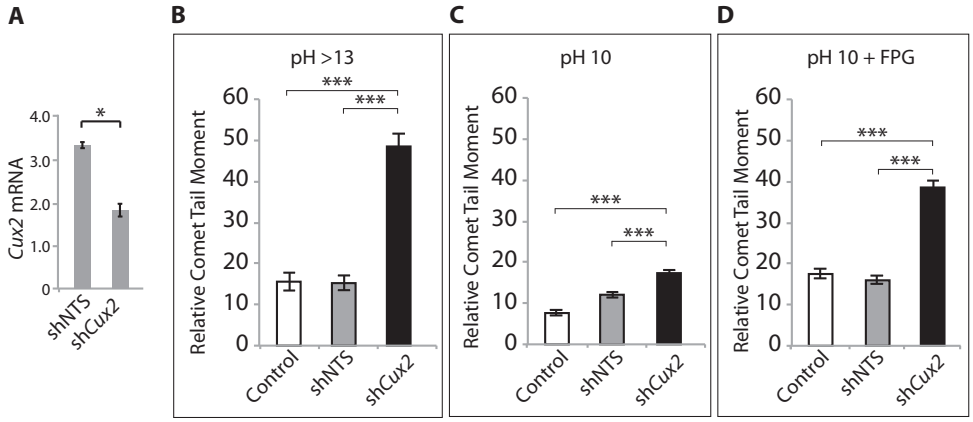

FIGURE 1. ***Cux2* knockdown increases DNA damage in embryonic cortical neurons.** Rat cortical neurons were infected with lentiviral vectors expressing *Cux2* shRNA or control non-targeting sequence (*NTS*). On day 4, RNA was isolated, and cells were submitted to single cell gel electrophoresis in various conditions. Comet tail moments were scored for at least 50 cells per condition. *Error bars* represent S.E. *, $p < 0.05$; ***, $p < 0.001$, Student's *t* test. *A*, RT-PCR analysis of *Cux2* mRNA levels. *B*, comet assays in alkaline conditions (pH > 13). *C*, comet assays at pH 10. *D*, comet assays at pH 10 following treatment with formamidopyrimidine-DNA glycosylase (*FPG*).

nol blue and 0.05% xylene cyanol) was added prior to loading on the gel. The DNA was loaded on a prewarmed 20% polyacrylamide-urea gel (19:1) and separated by electrophoresis in Tris borate and EDTA, pH 8.0 at constant 20 mA. To detect any uncleaved abasic DNA product produced by the glycosylase reaction, samples were further incubated for 30 min with 100 mM NaOH prior to loading on the gel.

In Vitro 8-OxoG Fluorogenic Cleavage Assay—The fluorogenic assay was performed with 100 nM double-stranded 16-mer deoxyoligonucleotides (Midland) as described (74). The top strand contains at its 5′-end a fluorescent reporter, carboxytetramethylrhodamine and an 8-oxoguanine residue at position 6. The other strand contains the Black Hole Quencher-2 at its 3′-end such that the quencher resides next to the fluorescent reporter after annealing of the two strands. Following cleavage by OGG1, a short deoxyoligonucleotide fluorophore-labeled product is spontaneously released from the remaining DNA fragment possessing the quencher, causing the fluorophore emission to increase. Cleavage reactions were conducted using 50 nM hOGG1 (New England Biolabs); various concentrations of BSA or the indicated bacterially purified His-tagged proteins in 50 mM NaCl, 10 mM Tris, pH 7.5, and 10 mM $MgCl_2$; and 100 nM fluorogenic double-stranded oligonucleotides containing an 8-oxoG base. The reactions were incubated at 37 °C, and fluorescence data were collected on RotorGene 3000 (Corbett Life Science) equipped with standard optics (excitation filter, 530 nm; emission filter, 580 nm). A linear regression model was used to determine the initial velocity of each enzymatic activity curve. The effects of each cut repeat and other proteins in the presence of 50 nM OGG1 were determined from nonlinear regression of initial velocity *versus* concentration of proteins using Prism 6.0 (GraphPad).

Electrophoretic Mobility Shift Assay (EMSA)—EMSAs were performed as described previously (75). Bacterially purified proteins (50 nM) were used in the reaction together with 60 ng of poly(dI-dC) as a nonspecific competitor DNA.

Results

Cux2 Knockdown Increases DNA Damage in Embryonic Cortical Neurons—Cux2 is expressed primarily in neuronal tissues during development and continues to be expressed in postmitotic neurons (61, 66). As a first step to investigate whether CUX2 plays a role in the repair of oxidative DNA damage, we tested whether the level of DNA damage would change in cortical neurons following the knockdown of *Cux2*. Cortical neurons were isolated from 17.5-day-old rat embryos and plated on a poly-D-lysine-coated tissue culture dish. The next day, neurons were infected with lentiviruses expressing *Cux2* shRNA or a non-targeting sequence as a control. On day 4, neurons were harvested and submitted to single cell gel electrophoresis in various conditions. Comet assays in alkaline conditions (pH > 13) detect double strand and single strand breaks as well as abasic sites and several types of altered bases that are intrinsically labile at high pH. Comet assays performed at pH 10 only detect double strand breaks and single strand breaks. Prior treatment with formamidopyrimidine-DNA glycosylase allows the detection of specific types of oxidized bases including 8-oxoG, formamidopyrimidines, and a number of oxidized purines. Infection of neurons with the lentivirus that expresses the non-targeting sequence did not appreciably affect levels of DNA damage (Fig. 1, *B*, *C*, and *D*). In contrast, the partial *Cux2* knockdown caused a significant increase in DNA damage in all conditions (Fig. 1). In particular, the drastic increase observed at pH 10 after treatment with formamidopyrimidine-DNA glycosylase indicates that the level of oxidized bases is increased when CUX2 expression is reduced (Fig. 1*D*).

Genetic Inactivation of Cux2 Reduces DNA Repair Efficiency in Mouse Embryo Fibroblasts—We then measured DNA damage in MEFs isolated from $Cux2^{-/-}$ and $Cux2^{+/+}$ mice (62). Levels of DNA damage were significantly higher in $Cux2^{-/-}$ MEFs as compared with wild type MEFs (Fig. 2, *B*, *C*, and *D*). Higher DNA damage in $Cux2^{-/-}$ MEFs, in particular oxidative DNA damage, could result from a higher production of ROS, lower expression of ROS scavengers, or reduced DNA repair capability. To compare the DNA repair efficiency of $Cux2^{-/-}$

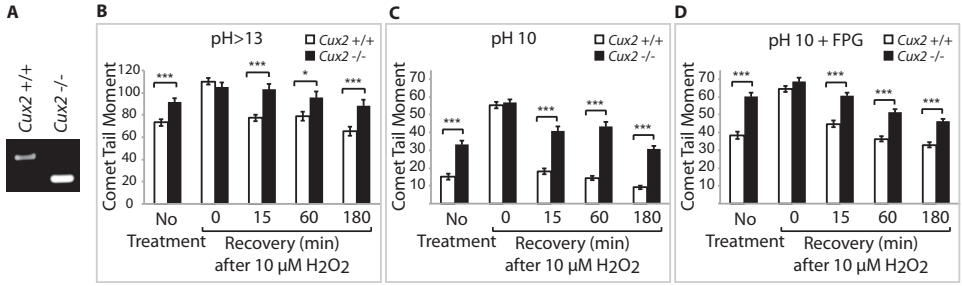

FIGURE 2. ***Cux2*$^{-/-}$ mouse embryo fibroblasts exhibit a defect in DNA repair.** MEFs from *Cux2*$^{+/+}$ and *Cux2*$^{-/-}$ mice were maintained in 3% oxygen, then exposed to 10 μM H_2O_2 for 20 min, allowed to recover for the indicated time, and then submitted to single cell gel electrophoresis. Comet tail moments were scored for at least 50 cells per condition. *Error bars* represent S.E. *, $p < 0.05$; ***, $p < 0.001$, Student's *t* test. *A*, PCR analysis of the *Cux2* knockdown mutation in the MEFs. *B*, comet assays in alkaline conditions (pH > 13). *C*, comet assay performed at pH 10. *D*, comet assay performed at pH 10 following treatment with formamidopyrimidine-DNA glycosylase (*FPG*).

and *Cux2*$^{+/+}$ MEFs, cells were treated with H_2O_2 and allowed to recover for various periods of time before assessing DNA damage. *Cux2*$^{-/-}$ MEFs exhibited a delay in the repair of DNA damage caused by H_2O_2 (Fig. 2, *B*, *C*, and *D*).

Cut Repeat Domains of CUX2 Stimulate the Glycosylase and AP Lyase Activities of OGG1—The first enzymatic steps of BER can be reproduced *in vitro* using purified OGG1 proteins. We first performed assays using radioactively labeled deoxyoligonucleotides that contain an 8-oxoG residue at position 16 of a 31-mer sequence. In this assay, treatment of DNA with NaOH at the end of the reaction generates a single strand break at the apurinic site generated by OGG1. Following separation by PAGE, quantification of the DNA substrate and product provides a measurement of OGG1 DNA glycosylase activity. In the absence of NaOH treatment, however, cleavage of DNA is entirely dependent on the AP lyase activity of OGG1, and the assay therefore measures both the glycosylase and AP lyase activities of OGG1. The reactions were performed in the presence of BSA as a control or various CUX2 recombinant proteins containing CR1, CR2, CR3HD, CR2CR3HD, or CR1CR2. A diagram of the proteins is shown in Fig. 3*A*, and a Coomassie stain is shown in Fig. 3*B*. Cleavage assays in the absence of OGG1 ensured that the purified proteins did not carry a cleavage activity on their own even when tested at 400 nM (Fig. 3*C*, *lanes 6–8*, and data not shown). In the assays with NaOH treatment, the glycosylase activity of OGG1 was stimulated ~3-fold by CR3HD, CR1CR2, and CR2CR3HD and 2-fold or less by CR1 and CR2 as compared with the reaction in the presence of BSA (Fig. 3*D*, compare BSA in *lane 8* with *lanes 1*, *2*, *5*, *6*, and *7*). In the absence of NaOH treatment, the AP lyase activity of OGG1 was also stimulated ~3-fold by CR3HD, CR1CR2, and CR2CR3HD as compared with the BSA lane (Fig. 3*D*, compare *lane 11* with *lanes 12*, *13*, and *14*). In contrast, CR1, CR2, and HOXB3 did not significantly affect the efficiency of the reaction (Fig. 3*D*, compare *lane 11* with *lanes 15*, *17*, and *18*).

As an alternative assay, we used deoxyoligonucleotides in which the top strand contains a fluorescent reporter at its 5′-end and an 8-oxoguanine residue at position 6 and the bottom strand contains a quencher at its 3′-end (Fig. 4*A*). In this assay, the glycosylase and AP lyase activities of OGG1 release a short fluorophore-labeled product. Measuring fluorescence emission over time enabled us to monitor the effect of increasing the concentration of various proteins while keeping the concentration of OGG1 to 50 nM. The results show that OGG1 is not affected by the addition of 50 nM BSA but is stimulated by the amount of various Cut repeat proteins (Fig. 4*B*). At higher concentration (400 nM), both BSA and HOXB3 increased the efficiency of the reaction to the same extent, an effect that is most likely attributable to the increased stability of OGG1 (Fig. 4*C*). At the same concentration, the Cut repeats further increased efficiency of the cleavage reaction (Fig. 4, *B* and *C*). Plotting enzymatic activity *versus* increasing concentration of added proteins showed that near maximal enzymatic activity was reached when 200 nM Cut repeat proteins were added (Fig. 4*D*). Among CUX2 recombinant proteins, the highest stimulation was achieved with CR3HD, CR1CR2, and CR2CR3HD, whereas more modest stimulation was observed with CR1 or CR2. Replacement of two amino acids facing outward within the first helix of CR1 as predicted from structural analysis of a Cut repeat (Protein Data Bank code 1X2L) reduced enzymatic activity almost to the level observed with BSA and HOXB3 (Fig. 4, *B*, *C*, and *D*). A more extensive mutational analysis of Cut repeats should reveal the regions and specific amino acids that are required for the stimulation of OGG1. Finally, CR1CR2 proteins derived from CUX1 or CUX2 exhibited similar stimulatory activity on OGG1, suggesting that the two proteins fulfill a similar function in DNA repair (Fig. 4*E*).

CUX2 Interacts Directly with OGG1 and Stimulate Its Binding to DNA Containing 8-OxoG—CUX2 carrying an HA epitope tag at its carboxyl terminus was detected in the immunoprecipitate obtained using an antibody against OGG1 (Fig. 5*A*, *lane 2*). Pulldown assays established that the two proteins were able to engage in a direct interaction. First, beads bound to His-CR1CR2 specifically pulled down purified OGG1 (Fig. 5*B*, *lane 2*). Second, beads bound to GST-OGG1 specifically pulled down purified His-CR1CR2 and His-CR3HD, whereas control beads did not (Fig. 5*C*, *lane 3*).

In a previous study, the Cut repeat domains of CUX1 were found to stimulate the binding of OGG1 specifically to DNA that contains an 8-oxoG. Interestingly, this effect on OGG1 did not require that the Cut repeat protein itself form a stable complex with DNA (52). To test whether the Cut repeats from CUX2 have the same effect on OGG1, we performed EMSAs using oligonucleotides that contain an 8-oxoG. CR1CR2, CR2CR3HD, and CR3HD all stimulated the binding of OGG1 to the probe containing an 8-oxoG (Fig. 5*D*, compare *lanes 2*

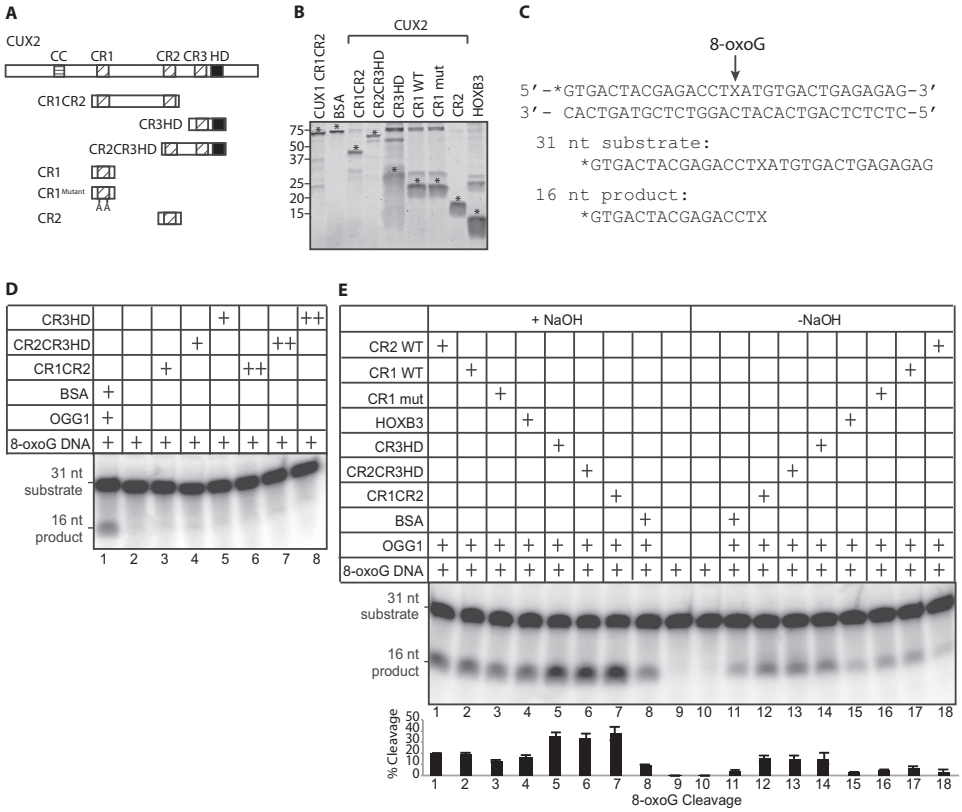

FIGURE 3. **Cut repeat domains of CUX2 stimulate the glycosylase and AP lyase activities of OGG1.** *A*, diagrammatic representation of CUX2 proteins. Shown at the *top* are the evolutionarily conserved domains: coiled coil (*CC*), CR1, CR2, CR3, and HD. $CR1^{Mut}$ contains two point mutations replacing glutamic acid with alanine. *B*, recombinant CUX2 proteins were expressed in bacteria, purified by affinity chromatography, separated by SDS-PAGE, and stained with Coomassie Blue. CUX2 proteins are indicated with an *asterisk*. *C*, double-stranded oligonucleotides containing an 8-oxoG were radioactively end-labeled (indicated by *stars*) and used in cleavage assays shown in *D* and *E*. Sequences of substrate and product are shown. *D*, 8-oxoG cleavage assay was performed for 30 min using 50 nM purified hOGG1 and 50 nM BSA in *lane 1*. In *lanes 3–8*, the assay was performed in the absence of OGG1 and with 50 nM (+) or 400 nM (++) of Cut repeat proteins only as indicated. Reactions were stopped, and DNA was submitted to NaOH treatment. *E*, double-stranded oligonucleotides containing an 8-oxoG were radioactively end-labeled and used in cleavage assays. Sequences of substrate and product are shown. The 8-oxoG cleavage assay was performed for 30 min using 50 nM purified hOGG1 and BSA or bacterially purified proteins as indicated. Reactions were stopped, and DNA was submitted to NaOH treatment or not (+ or − *NaOH*). As NaOH cleaves DNA at apyrimidinic sites, assays in the presence of NaOH monitor OGG1 glycosylase activity only, whereas assays in the absence of NaOH monitor both OGG1 glycosylase and AP lyase activities. *Error bars* represent S.E. *nt*, nucleotides.

and *3*, *lanes 6* and *7*, and *lanes 10* and *11*). However, only CR2CR3HD was able to bind with high affinity to the probe (Fig. 5*D*, *lane 12*). In contrast, only very weak bands can be observed in the lanes with CR1CR2 or CR3HD, there is no reduction in the intensity of the free probe, and there is no intense smear that could indicate unstable binding (Fig. 5*D*, *lanes 4* and *8*). These results indicate that high affinity DNA binding is not required for a Cut repeat protein to stimulate the binding of OGG1 to 8-oxoG. Moreover, we note that the mobility of the complex produced by OGG1 was not altered in the presence of CR2CR3HD or any other Cut repeats, suggesting that OGG1 and Cut repeats do not form a stable ternary complex with DNA.

Ectopic Expression of CUX2 Proteins Rescues the DNA Repair Defect of Cux2$^{-/-}$ MEFs—We wanted to verify whether the CUX2 peptides that stimulate OGG1 in the *in vitro* 8-oxoG cleavage assay would be able to rescue the DNA repair defect of *Cux2*$^{-/-}$ MEFs. A nuclear localization signal (NLS) was added to each peptide to ensure that the Cut repeats would be targeted to the nucleus, and an HA epitope tag was also included to facilitate detection. Retroviral infections were performed to obtain a population of *Cux2*$^{-/-}$ MEFs stably expressing CR1CR2, CR2CR3HD, CR3HD, or the *lacZ* gene as a control (Fig. 6*A*). Comet assays performed in various conditions showed that DNA damage was reduced by ectopic expression of each of the three recombinant CUX2 proteins (Fig. 6, *B*, *C*, and *D*).

CUX2 Knockdown Reduces Proliferation and Increases Apoptosis in HCC38 Breast Tumor Cells—A recent genome-wide shRNA screen identified *CUX2* as an essential gene in a number of breast tumor cell lines (76). For example, *CUX2* was ranked the 183rd essential gene in the HCC38 breast tumor cell line. To validate these results, we independently infected HCC38 cells with retroviruses expressing *CUX2* shRNAs or luciferase shRNA as a control and monitored cell proliferation using the WST-1 assay as well as the IncuCyte live cell imaging system. RT-PCR analysis indicated that *CUX2* expression was partially knocked down (Fig. 7*A*), whereas both proliferation assays showed that *CUX2* shRNA-infected HCC38 cells stopped proliferating after 1 or 2 days (Fig. 7, *B* and *C*). On day 2, cells were analyzed by flow cytometry using 7-AAD and annexin V as markers of cell death and apoptosis, respectively. The population of HCC38 cells that received the *CUX2* shRNA displayed a significant decrease in the proportion of live cells negative for

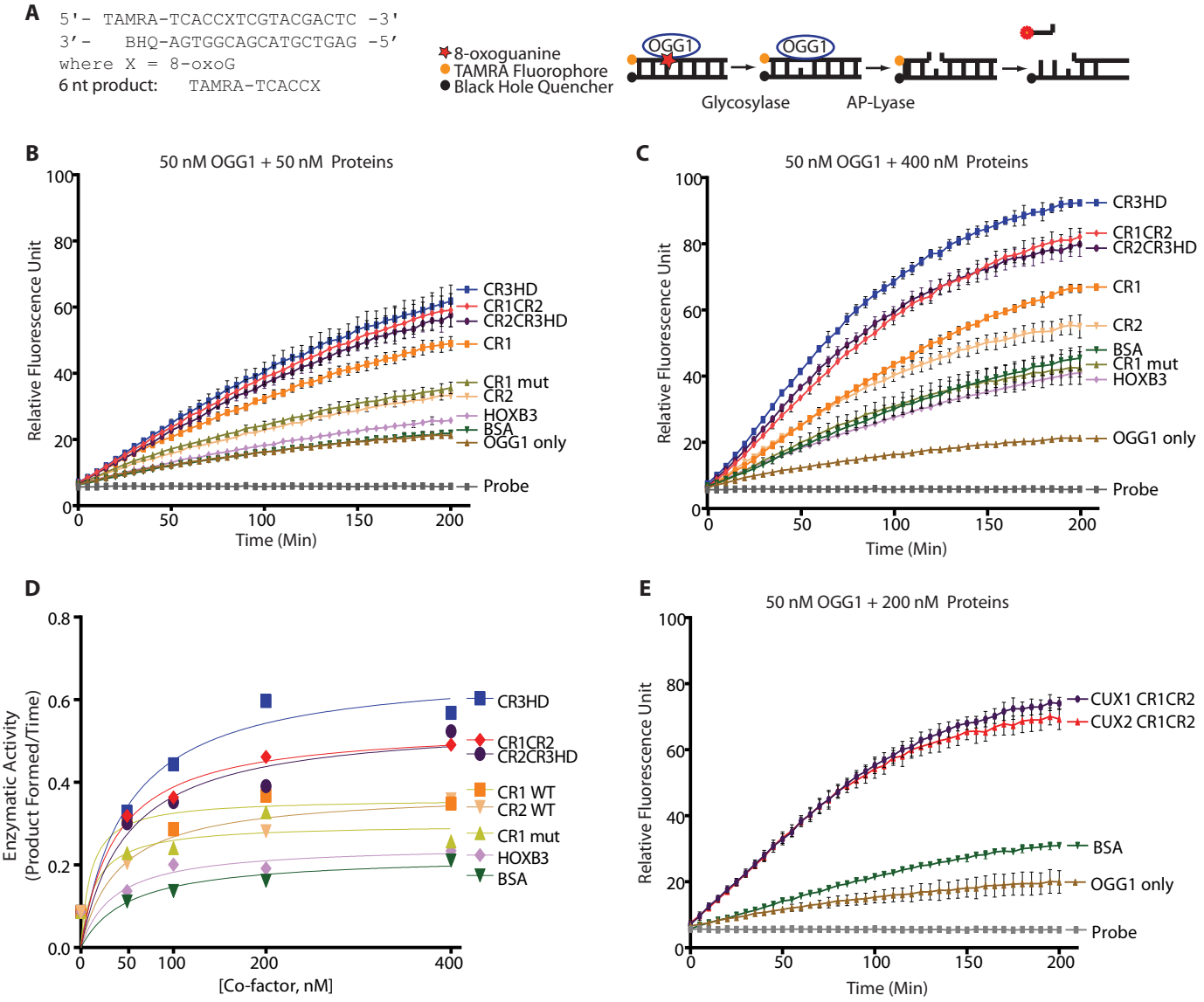

FIGURE 4. **Stimulation of enzymatic activity of OGG1 by CUX2 Cut repeat domains.** *A*, schematic representation of the 8-oxoG fluorescence-based cleavage assay. The *top* strand contains the carboxytetramethylrhodamine (*TAMRA*) fluorescent reporter at its 5′-end and an 8-oxoguanine residue at position 6. The *bottom* strand contains the Black Hole Quencher-2 (*BHQ*) at its 3′-end. The glycosylase and AP lyase activities of OGG1 release a short fluorophore-labeled product. *B*, cleavage activity of 50 nM OGG1 monitored over 200 min in the presence of 50 nM BSA, HOXB3, or various CUX2 cut repeats. *C*, cleavage activity of 50 nM OGG1 monitored over 200 min in the presence of 400 nM BSA, HOXB3, or various CUX2 cut repeats. *D*, OGG1 enzymatic activity was determined using initial velocity of OGG1 activity from time-dependent curves using 50 nM OGG1 and four different concentrations (50, 100, 200, and 400 nM) of BSA, HOXB3, or various CUX2 cut repeats. *E*, cleavage activity of 50 nM OGG1 monitored over 200 min in the presence of 200 nM BSA, CUX1 CR1CR2, or CUX2 CR1CR2. *Error bars* represent S.D.

both markers (63 *versus* 88.5%) and a corresponding increase in early apoptotic cells (7-AAD-negative, annexin V-positive, 7 *versus* 1.2%) and in late apoptotic cells positive for both markers (22.5 *versus* 4.3%) (Fig. 7*D*). Similar results were obtained with a retrovirus expressing a different *CUX2* shRNA (data not shown). These findings indicate that a partial *CUX2* knockdown in HCC38 breast tumor cells causes a proliferation arrest associated with apoptotic cell death.

CUX2 Knockdown Delays Repair of Oxidative DNA Damage—Single cell gel electrophoresis assays showed an increase in DNA damage in HCC38 cells that received the *CUX2* shRNA vector (Fig. 8, *A*, *B*, and *C*). To monitor directly the repair of oxidative DNA damage, cells were treated with H_2O_2 and allowed to recover for various periods of time. We observed a significant delay in the repair of oxidative DNA damage in HCC38 cells infected with the *CUX2* shRNA vector (Fig. 8, *A*, *B*, and *C*).

Ectopic Expression of CUX2 Proteins Accelerates DNA Repair—CUX2 is not normally expressed in mammary epithelial cells. The effects of *CUX2* knockdown in HCC38 breast tumor cells suggest that higher CUX2 expression, albeit still very modest, may be selected in some tumor cells because CUX2 helps these cells to cope with higher ROS levels. To verify this hypothesis, we prepared populations of HCC38 cells stably expressing CUX2 recombinant proteins containing CR1CR2 or CR2CR3HD or the *lacZ* gene as a control (Fig. 9*A*). Comet assays showed that ectopic expression of either CR1CR2 or CR2CR3HD reduced the steady-state level of DNA damage

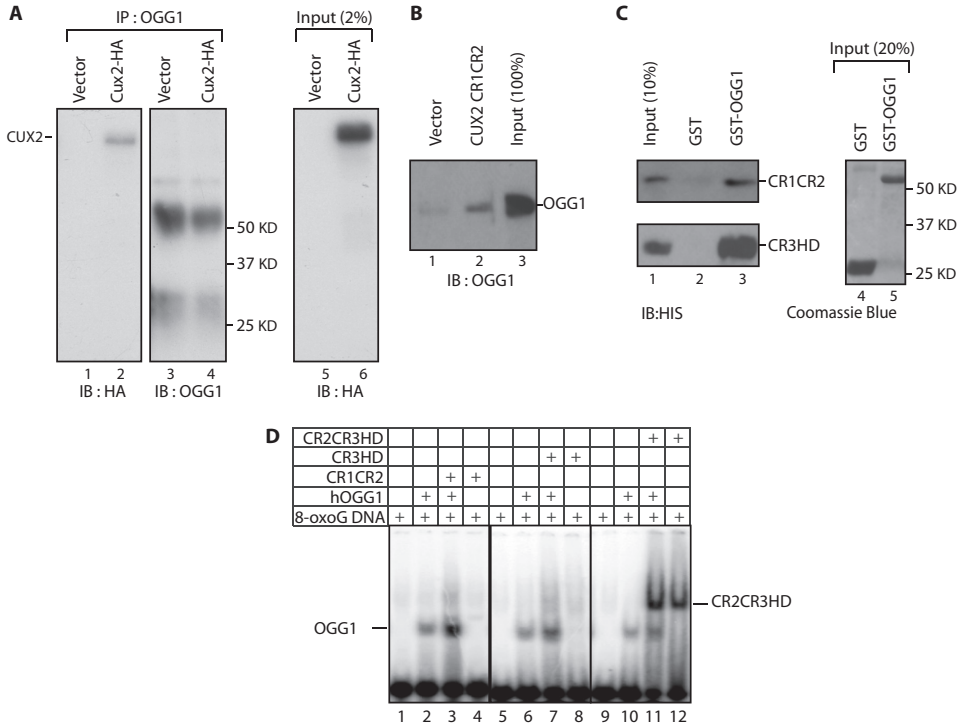

FIGURE 5. **CUX2 interacts directly with OGG1 and stimulates its binding to DNA.** *A*, HEK293T cells were transiently transfected with an empty vector or a vector expressing CUX2-HA. Total protein extracts were subjected to immunoprecipitation (*IP*) with OGG1 antibody and analyzed by immunoblotting (*IB*) with an HA antibody. Input (2%) was loaded as a protein expression control. *B*, a pulldown assay was performed using 100 ng of purified GST-OGG1 and beads bound to His-tagged CUX2-CR1CR2 or beads incubated with an extract from bacteria containing the empty vector. Following separation by SDS-PAGE, immunoblotting was performed with anti-OGG1 antibody. *C*, a pulldown assay was performed using 400 ng of purified His-tagged CUX2-CR1CR2 and CR3HD with glutathione beads bound to either GST alone or GST-OGG1. Following separation by SDS-PAGE, immunoblotting was performed with anti-His antibody. Equal loading of GST and GST-OGG1 was verified by Coomassie Blue staining. *D*, EMSA was performed using oligonucleotides containing an 8-oxoG and purified hOGG1 in the presence or absence of a CUX1 peptide as indicated.

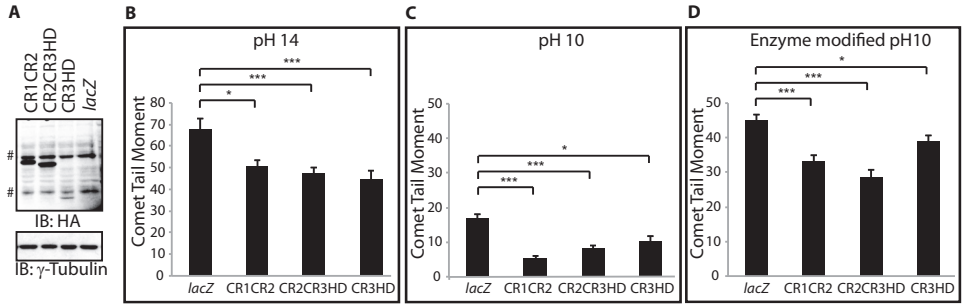

FIGURE 6. **Ectopic expression of CUX2 proteins rescues the DNA repair defect of *Cux2*$^{-/-}$ MEFs.** *Cux2*$^{-/-}$ MEFs were stably infected with retroviruses expressing CUX2 CR1CR2-NLS-HA, CUX2 CR2CR3HD-NLS-HA, CUX2 CR3HD-NLS-HA, or *lacZ* (control). Protein extracts were prepared, and cells were submitted to single cell gel electrophoresis in various conditions as in Fig. 1. *A*, expression of recombinant CUX2 protein was analyzed by immunoblotting (*IB*) using HA antibody. # indicates nonspecific bands. *B*, comet assays in alkaline conditions (pH > 13). *C*, comet assays at pH 10. *D*, comet assays at pH 10 following treatment with formamidopyrimidine-DNA glycosylase. *Error bars* represent S.E. *, $p < 0.05$; ***, $p < 0.001$, Student's *t* test.

(Fig. 9*B*, *No Treatment*) and accelerated repair of DNA damage following treatment with H_2O_2 (Fig. 9*B*). Together, these results indicate that higher CUX2 expression in breast tumor cells accelerates DNA repair and reduces DNA damage.

Discussion

Experimental evidence supporting the role of CUX2 as an accessory factor that stimulates the repair of oxidative DNA damage can be summarized as follows. CUX2 knockdown increased oxidative DNA damage in cortical neurons and in HCC38 breast tumor cells (Figs. 1 and 8). *Cux2*$^{-/-}$ MEFs exhibited a delay in the repair of oxidative DNA damage as compared with *Cux2*$^{+/+}$ MEFs (Fig. 2). Similarly, *CUX2* knockdown caused a delay in the repair of oxidative DNA damage in HCC38 cells (Fig. 8). *In vitro*, we showed that CUX2 recombinant proteins containing various combinations of Cut repeat domains were able to stimulate the binding of OGG1 to 8-oxoG-containing DNA and to stimulate both the glycosylase and AP lyase enzymatic activities of OGG1 (Figs. 3 and 4). Cux2 proteins were shown to interact in co-immunoprecipitation and pulldown assays (Fig. 5). Finally, ectopic expression of CUX2 recombinant proteins rescued the DNA repair defect of *Cux2*$^{-/-}$ MEFs and accelerated DNA repair in HCC38 cells (Figs. 6 and 9). Together, these results build a strong case to support a direct role of CUX2 in base excision repair.

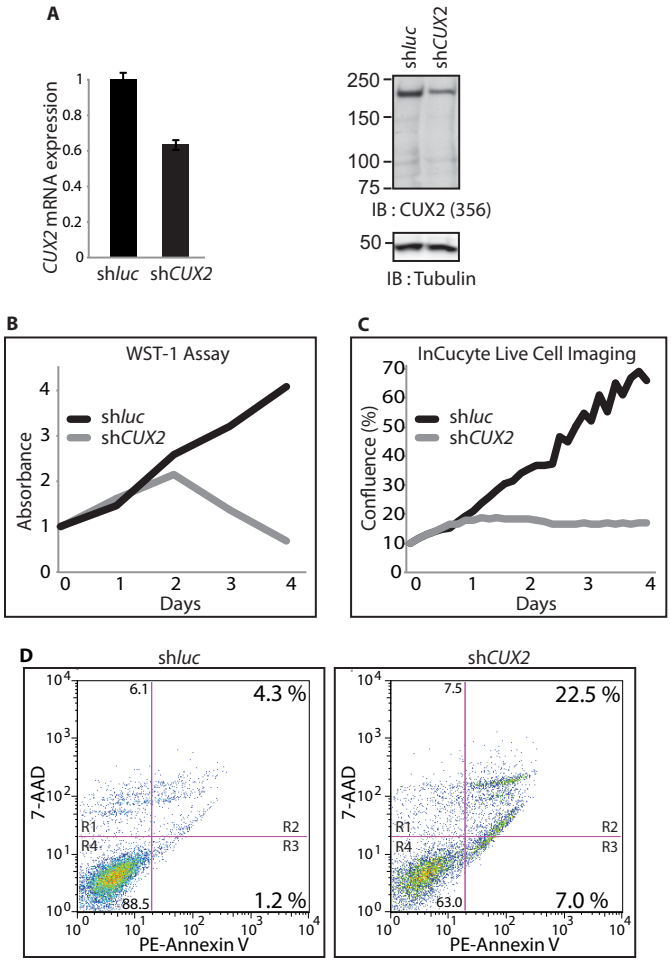

FIGURE 7. ***CUX2* knockdown reduces proliferation and increases apoptosis in HCC38 breast tumor cells.** HCC38 breast tumor cells were infected with lentiviruses expressing shCUX2 or shLuciferase (*shLUC*) RNA. *A*, *CUX2* mRNA and protein expression were measured on day 2 by RT-PCR and immunoblotting (*IB*). *Error bars* represent S.D. *B*, cell viability was assessed using the WST-1 assay. *C*, cell proliferation was measured using the IncuCyte live cell imaging system. *D*, on day 2, apoptosis was monitored using phycoerythrin (*PE*)-conjugated recombinant human annexin V and 7-AAD and analyzed by flow cytometry. Dot plots were generated from 10,000 analyzable events. *R1* represents annexin V-negative and 7-AAD-positive dead cells; *R2* represents late apoptotic cells positive for both annexin V binding and 7-AAD uptake; *R3* represents early apoptotic cells positive for annexin V and negative for 7-AAD, demonstrating cytoplasmic membrane integrity; and *R4* represent annexin V- and 7-AAD-negative viable cells.

Similar experimental evidence previously established the role of CUX1 in base excision repair (52). Following duplication of the ancestral CUX gene, CUX1 and CUX2 have evolved distinct patterns of gene expression and acquired unique molecular functions. Although CUX1 is expressed in most if not all tissues, CUX2 adopted a more restricted profile of expression predominantly in neuronal cells (49, 57, 58, 62). In contrast to CUX2, CUX1 is regulated in a cell cycle-dependent manner, and a shorter CUX1 isoform functions as a transcriptional factor that promotes many processes associated with cell cycle progression (68, 69). Despite their divergent evolution, CUX1 and CUX2 exhibit high sequence conservation within specific protein regions, notably in the Cut repeat domains, and have conserved similar molecular functions (48, 49). Both CUX1 and CUX2 continue to be expressed in the brain where they fulfill additive and complementary functions in neuronal cell type specification (Refs. 42 and 43; for a review, see Ref. 46). Based on our results, we suggest that both CUX1 and CUX2 must also play important roles in the repair of oxidative DNA damage in the brain. The human brain extracts ~50% of the oxygen and 10% of the glucose from the arterial blood (77). Indeed, neurons have very high rates of oxygen metabolism due to their high glucose requirement and the dependence on aerobic oxidation of glucose as their source of energy (78). Combined with the low level of antioxidant enzymes in the brain, the type of DNA damage most likely to occur in the neuronal cells is ROS-induced oxidative DNA damage (79, 80). In this context, it is tempting to speculate that duplication of the CUX gene may have been selected during evolution in part because of the protection conferred by CUX proteins against oxidative DNA damage.

The p110 CUX1 isoform was previously shown to play an important role in directly stimulating the expression of many genes involved in the DNA damage response (81). Therefore, we cannot exclude the possibility of a transcriptional effect in experiments where we documented the impact of CUX2 knockdown or overexpression. However, we consider it unlikely that CUX2 could play a similar role as CUX1 in the regulation of DNA damage response genes. First, a CUX2 isoform that is equivalent to p110 CUX1 has not been identified (67). Second, extensive global gene expression analysis following CUX2 overexpression and CUX2 knockdown has not revealed any difference in the expression of DNA damage response genes (59).

We found that the Cut repeat domains of CUX2 can interact with OGG1 (Fig. 5, *B* and *C*), increase the binding of OGG1 to deoxyoligonucleotides containing an 8-oxoG (Fig. 5*D*), and stimulate the enzymatic activities of OGG1 (Figs. 3 and 4). However, some Cut repeat proteins that stimulated OGG1 did not themselves bind with high affinity to the DNA (Fig. 5*D*, CR1CR2 and CR3HD, *lanes 4* and *8*), whereas one protein that could form a strong retarded complex, CR2CR3HD (Fig. 5*D*, *lane 12*) still did not form a ternary complex with OGG1 and DNA (Fig. 5*D*, *lane 11*). Similar observations were previously made with the Cut repeats of CUX1 (52). These findings suggest that the mechanism by which Cut repeats stimulate OGG1 may involve a transient interaction between the two proteins. Cut repeats may facilitate an allosteric change in OGG1, a notion consistent with structural studies reporting conformational transitions of OGG1 associated with its biochemical activities (Refs. 83–86; for a review, see Ref. 87). Alternatively, Cut repeats may transiently alter the conformation of DNA to facilitate the recognition of 8-oxoG by OGG1 or help OGG1 distort DNA while searching for damaged bases (88). A mechanism of action involving transient alteration of DNA conformation is consistent with the extremely fast DNA binding kinetics of some Cut repeats (71).

We have previously reported that the role of CUX1 in base excision repair is exploited by cancer cells that produce elevated levels of ROS (53). High CUX1 expression prevents RAS-induced senescence and enables the development of RAS-driven tumors (53). Moreover, CUX1 knockdown is synthetic lethal to RAS-transformed cells (53, 54). The acute dependence of RAS-driven tumor cells on CUX1 expression illustrates a

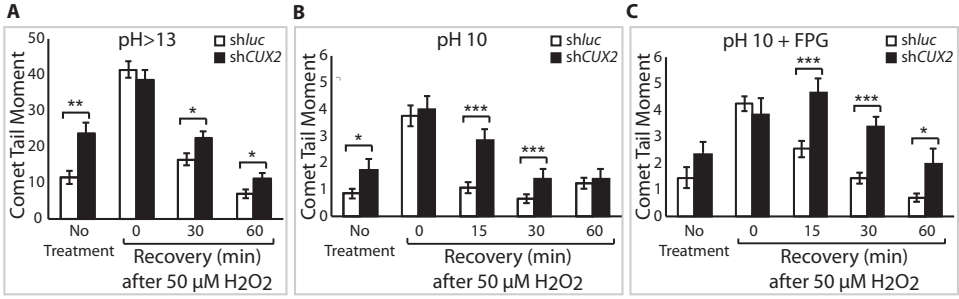

FIGURE 8. ***CUX2* knockdown delays repair of oxidative DNA damage.** HCC38 breast tumor cells were infected with lentiviruses expressing shCUX2 or shLuciferase (*sh Luc*) RNA. Following exposure to 50 μM H_2O_2, cells were allowed to recover for the indicated time and then submitted to single cell gel electrophoresis in various conditions to quantify DNA damage. *A*, comet assays in alkaline conditions (pH > 13). *B*, comet assays at pH 10. *C*, comet assays at pH 10 following treatment with formamidopyrimidine-DNA glycosylase (*FPG*). Comet tail moments were scored for at least 50 cells per condition. *Error bars* represent S.E. *, $p < 0.05$; **, $p < 0.01$; ***, $p < 0.001$, Student's *t* test.

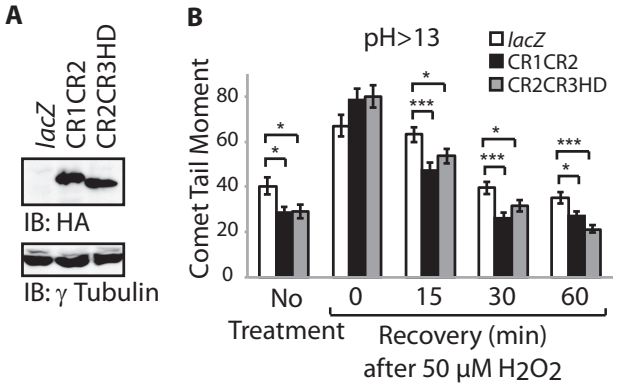

FIGURE 9. **Ectopic expression of CUX2 proteins accelerates DNA repair.** HCC38 cells were stably infected with retroviruses expressing CUX2 CR1CR2-NLS-HA, CUX2 CR2CR3HD-NLS-HA, or nothing (vector). *A*, expression of recombinant CUX2 protein expression was analyzed by immunoblotting (*IB*) using HA antibody. *B*, following exposure to 50 μM H_2O_2, cells were allowed to recover for the indicated time and then submitted to single cell gel electrophoresis as described in Fig. 2. Comet tail moments were scored for at least 50 cells per conditions. *Error bars* represent S.E. *, $p < 0.05$; ***, $p < 0.001$, Student's *t* test.

case of non-oncogene addiction whereby cancer cells are dependent on the heightened activity of a protein that is not itself an oncogene (55, 56). The findings that *CUX2* knockdown also is detrimental to some breast tumor cells suggests that higher expression of any CUX gene may be selected in cancer cells that sustain high ROS levels (76). It should be noted that CUX1 was not identified in this particular screen likely because three of the five *CUX1* shRNAs were targeted not to CUX1 but to the CUX1 alternatively spliced product (CASP) mRNA in the 80K library developed by The RNAi Consortium (89). The identification of *CUX1* or *CUX2* in independent screens for synthetic lethal interactions in cancer cells suggests that adaptation to the particular metabolism of cancer cells will likely involve selection for higher expression of various ROS scavengers as well as proteins that play a role in the repair of oxidative DNA damage. In this regard, it is remarkable that the genome-wide screen for synthetic lethal interactions with the KRAS oncogene uncovered four other genes involved in base excision repair: NEIL2, XRCC1, DNA polymerase β, and LIG3 (54). Together, these findings indicate that, contrary to the notion that cancer cells only exhibit defects in DNA repair mechanisms, in fact some cancer cells exhibit a very efficient base excision repair pathway.

Author Contributions—R. P. designed, performed, and analyzed the experiments shown in Figs. 2; 5, *A*, *B*, and *D*; 6; 7; 8; and 9. Z. M. R. designed, performed, and analyzed the experiments shown in Figs. 1, 3, 4, 6, and 8 and wrote the paper. S. K. designed, performed, and analyzed the experiment shown in Fig. 5*C*. P. M. D. designed, performed, and analyzed the experiments shown in Fig. 1. R. M. designed, performed, and analyzed the experiments shown in Fig. 7. L. L. designed, performed, and analyzed the experiments shown in Figs. 3 and 5*D*. S. D. analyzed the experiments shown in Figs. 2, 6, 8, and 9. N. L.-V. designed, performed, and analyzed the experiments shown in Fig. 1. A. I designed, performed, and analyzed the experiments shown in Figs. 2 and 6. A. N. conceived and coordinated the study and wrote the paper. All authors reviewed the results and approved the final version of the manuscript.

Acknowledgments—We are grateful to Drs. N. Noren Hooten and M. K. Evans (GST-OGG1) and Dr. G. Sauvageau (His-HOXB3) for generously providing plasmids. We are indebted to Drs. T. Paz-Elizur and Z. Livneh for the protocol on cleavage assays. Infrastructure support and technical assistance were made possible with funds from the Canadian Foundation for Innovation and the Ministère du Développement économique, innovation et exportation Québec.

References

1. Friedberg, E. C., Walker, G. C., and Siede, W. (2006) *DNA Repair and Mutagenesis*, 2nd Ed., pp. 169–226, ASM Press, Washington, D. C.
2. Hamilton, M. L., Van Remmen, H., Drake, J. A., Yang, H., Guo, Z. M., Kewitt, K., Walter, C. A., and Richardson, A. (2001) Does oxidative damage to DNA increase with age? *Proc. Natl. Acad. Sci. U.S.A.* **98,** 10469–10474
3. Hirano, T., Yamaguchi, R., Asami, S., Iwamoto, N., and Kasai, H. (1996) 8-Hydroxyguanine levels in nuclear DNA and its repair activity in rat organs associated with age. *J. Gerontol. A Biol. Sci. Med. Sci.* **51A,** B303–B307
4. Kaneko, T., Tahara, S., and Matsuo, M. (1996) Non-linear accumulation of 8-hydroxy-2′-deoxyguanosine, a marker of oxidized DNA damage, during aging. *Mutat. Res.* **316,** 277–285
5. Nakae, D., Akai, H., Kishida, H., Kusuoka, O., Tsutsumi, M., and Konishi, Y. (2000) Age and organ dependent spontaneous generation of nuclear 8-hydroxydeoxyguanosine in male Fischer 344 rats. *Lab. Invest.* **80,** 249–261
6. Shen, S., Cooley, D. M., Glickman, L. T., Glickman, N., and Waters, D. J. (2001) Reduction in DNA damage in brain and peripheral blood lymphocytes of elderly dogs after treatment with dehydroepiandrosterone (DHEA). *Mutat. Res.* **480–481,** 153–162
7. Barja, G. (2004) Aging in vertebrates, and the effect of caloric restriction: a mitochondrial free radical production-DNA damage mechanism? *Biol. Rev.* **79,** 235–251
8. Englander, E. W. (2008) Brain capacity for repair of oxidatively damaged DNA and preservation of neuronal function. *Mech. Ageing Dev.* **129,** 475–482

9. Wilson, D. M., 3rd, and Bohr, V. A. (2007) The mechanics of base excision repair, and its relationship to aging and disease. *DNA Repair* **6,** 544–559
10. Wilson, D. M., 3rd, and McNeill, D. R. (2007) Base excision repair and the central nervous system. *Neuroscience* **145,** 1187–1200
11. Weissman, L., Jo, D. G., Sørensen, M. M., de Souza-Pinto, N. C., Markesbery, W. R., Mattson, M. P., and Bohr, V. A. (2007) Defective DNA base excision repair in brain from individuals with Alzheimer's disease and amnestic mild cognitive impairment. *Nucleic Acids Res.* **35,** 5545–5555
12. Hegde, M. L., Hazra, T. K., and Mitra, S. (2008) Early steps in the DNA base excision/single-strand interruption repair pathway in mammalian cells. *Cell Res.* **18,** 27–47
13. Grollman, A. P., and Moriya, M. (1993) Mutagenesis by 8-oxoguanine: an enemy within. *Trends Genet.* **9,** 246–249
14. Radicella, J. P., Dherin, C., Desmaze, C., Fox, M. S., and Boiteux, S. (1997) Cloning and characterization of hOGG1, a human homolog of the OGG1 gene of *Saccharomyces cerevisiae*. *Proc. Natl. Acad. Sci. U.S.A.* **94,** 8010–8015
15. Hazra, T. K., Izumi, T., Boldogh, I., Imhoff, B., Kow, Y. W., Jaruga, P., Dizdaroglu, M., and Mitra, S. (2002) Identification and characterization of a human DNA glycosylase for repair of modified bases in oxidatively damaged DNA. *Proc. Natl. Acad. Sci. U.S.A.* **99,** 3523–3528
16. Morland, I., Rolseth, V., Luna, L., Rognes, T., Bjørås, M., and Seeberg, E. (2002) Human DNA glycosylases of the bacterial Fpg/MutM superfamily: an alternative pathway for the repair of 8-oxoguanine and other oxidation products in DNA. *Nucleic Acids Res.* **30,** 4926–4936
17. Parsons, J. L., Zharkov, D. O., and Dianov, G. L. (2005) NEIL1 excises 3′ end proximal oxidative DNA lesions resistant to cleavage by NTH1 and OGG1. *Nucleic Acids Res.* **33,** 4849–4856
18. Demple, B., and Sung, J. S. (2005) Molecular and biological roles of Ape1 protein in mammalian base excision repair. *DNA Repair* **4,** 1442–1449
19. Wiederhold, L., Leppard, J. B., Kedar, P., Karimi-Busheri, F., Rasouli-Nia, A., Weinfeld, M., Tomkinson, A. E., Izumi, T., Prasad, R., Wilson, S. H., Mitra, S., and Hazra, T. K. (2004) AP endonuclease-independent DNA base excision repair in human cells. *Mol. Cell* **15,** 209–220
20. Caradonna, S. J., and Cheng, Y. C. (1982) DNA glycosylases. *Mol. Cell. Biochem.* **46,** 49–63
21. Lindahl, T. (1979) DNA glycosylases, endonucleases for apurinic/apyrimidinic sites, and base excision-repair. *Prog. Nucleic Acid Res. Mol. Biol.* **22,** 135–192
22. Campalans, A., Marsin, S., Nakabeppu, Y., O'connor, T. R., Boiteux, S., and Radicella, J. P. (2005) XRCC1 interactions with multiple DNA glycosylases: a model for its recruitment to base excision repair. *DNA Repair* **4,** 826–835
23. Marsin, S., Vidal, A. E., Sossou, M., Ménissier-de Murcia, J., Le Page, F., Boiteux, S., de Murcia, G., and Radicella, J. P. (2003) Role of XRCC1 in the coordination and stimulation of oxidative DNA damage repair initiated by the DNA glycosylase hOGG1. *J. Biol. Chem.* **278,** 44068–44074
24. Akbari, M., Solvang-Garten, K., Hanssen-Bauer, A., Lieske, N. V., Pettersen, H. S., Pettersen, G. K., Wilson, D. M., 3rd, Krokan, H. E., and Otterlei, M. (2010) Direct interaction between XRCC1 and UNG2 facilitates rapid repair of uracil in DNA by XRCC1 complexes. *DNA Repair* **9,** 785–795
25. Campalans, A., Moritz, E., Kortulewski, T., Biard, D., Epe, B., and Radicella, J. P. (2015) Interaction with OGG1 is required for efficient recruitment of XRCC1 to base excision repair and maintenance of genetic stability after exposure to oxidative stress. *Mol. Cell. Biol.* **35,** 1648–1658
26. Hill, J. W., Hazra, T. K., Izumi, T., and Mitra, S. (2001) Stimulation of human 8-oxoguanine-DNA glycosylase by AP-endonuclease: potential coordination of the initial steps in base excision repair. *Nucleic Acids Res.* **29,** 430–438
27. Vidal, A. E., Hickson, I. D., Boiteux, S., and Radicella, J. P. (2001) Mechanism of stimulation of the DNA glycosylase activity of hOGG1 by the major human AP endonuclease: bypass of the AP lyase activity step. *Nucleic Acids Res.* **29,** 1285–1292
28. Mokkapati, S. K., Wiederhold, L., Hazra, T. K., and Mitra, S. (2004) Stimulation of DNA glycosylase activity of OGG1 by NEIL1: functional collaboration between two human DNA glycosylases. *Biochemistry* **43,** 11596–11604
29. Das, S., Chattopadhyay, R., Bhakat, K. K., Boldogh, I., Kohno, K., Prasad, R., Wilson, S. H., and Hazra, T. K. (2007) Stimulation of NEIL2-mediated oxidized base excision repair via YB-1 interaction during oxidative stress. *J. Biol. Chem.* **282,** 28474–28484
30. Marenstein, D. R., Ocampo, M. T., Chan, M. K., Altamirano, A., Basu, A. K., Boorstein, R. J., Cunningham, R. P., and Teebor, G. W. (2001) Stimulation of human endonuclease III by Y box-binding protein 1 (DNA-binding protein B). Interaction between a base excision repair enzyme and a transcription factor. *J. Biol. Chem.* **276,** 21242–21249
31. Prasad, R., Liu, Y., Deterding, L. J., Poltoratsky, V. P., Kedar, P. S., Horton, J. K., Kanno, S., Asagoshi, K., Hou, E. W., Khodyreva, S. N., Lavrik, O. I., Tomer, K. B., Yasui, A., and Wilson, S. H. (2007) HMGB1 is a cofactor in mammalian base excision repair. *Mol. Cell* **27,** 829–841
32. Rai, K., Huggins, I. J., James, S. R., Karpf, A. R., Jones, D. A., and Cairns, B. R. (2008) DNA demethylation in zebrafish involves the coupling of a deaminase, a glycosylase, and gadd45. *Cell* **135,** 1201–1212
33. Li, Z., Gu, T.-P., Weber, A. R., Shen, J.-Z., Li, B.-Z., Xie, Z.-G., Yin, R., Guo, F., Liu, X., Tang, F., Wang, H., Schär, P., and Xu, G.-L. (2015) Gadd45a promotes DNA demethylation through TDG. *Nucleic Acids Res.* **43,** 3986–3997
34. Noren Hooten, N., Fitzpatrick, M., Kompaniez, K., Jacob, K. D., Moore, B. R., Nagle, J., Barnes, J., Lohani, A., and Evans, M. K. (2012) Coordination of DNA repair by NEIL1 and PARP-1: a possible link to aging. *Aging* **4,** 674–685
35. Noren Hooten, N., Kompaniez, K., Barnes, J., Lohani, A., and Evans, M. K. (2011) Poly(ADP-ribose) polymerase 1 (PARP-1) binds to 8-oxoguanine-DNA glycosylase (OGG1). *J. Biol. Chem.* **286,** 44679–44690
36. Bodmer, R., Barbel, S., Sheperd, S., Jack, J. W., Jan, L. Y., and Jan, Y. N. (1987) Transformation of sensory organs by mutations of the cut locus of D. melanogaster. *Cell* **51,** 293–307
37. Blochlinger, K., Bodmer, R., Jan, L. Y., and Jan, Y. N. (1990) Patterns of expression of cut, a protein required for external sensory organ development in wild-type and cut mutant *Drosophila* embryos. *Genes Dev.* **4,** 1322–1331
38. Grueber, W. B., Jan, L. Y., and Jan, Y. N. (2003) Different levels of the homeodomain protein cut regulate distinct dendrite branching patterns of *Drosophila* multidendritic neurons. *Cell* **112,** 805–818
39. Jinushi-Nakao, S., Arvind, R., Amikura, R., Kinameri, E., Liu, A. W., and Moore, A. W. (2007) Knot/Collier and cut control different aspects of dendrite cytoskeleton and synergize to define final arbor shape. *Neuron* **56,** 963–978
40. Komiyama, T., and Luo, L. (2007) Intrinsic control of precise dendritic targeting by an ensemble of transcription factors. *Curr. Biol.* **17,** 278–285
41. Moore, A. W. (2008) Intrinsic mechanisms to define neuron class-specific dendrite arbor morphology. *Cell Adh. Migr.* **2,** 81–82
42. Cubelos, B., Sebastián-Serrano, A., Kim, S., Redondo, J. M., Walsh, C., and Nieto, M. (2008) Cux-1 and Cux-2 control the development of Reelin expressing cortical interneurons. *Dev. Neurobiol.* **68,** 917–925
43. Cubelos, B., Sebastián-Serrano, A., Beccari, L., Calcagnotto, M. E., Cisneros, E., Kim, S., Dopazo, A., Alvarez-Dolado, M., Redondo, J. M., Bovolenta, P., Walsh, C. A., and Nieto, M. (2010) Cux1 and Cux2 regulate dendritic branching, spine morphology, and synapses of the upper layer neurons of the cortex. *Neuron* **66,** 523–535
44. Li, N., Zhao, C.-T., Wang, Y., and Yuan, X.-B. (2010) The transcription factor Cux1 regulates dendritic morphology of cortical pyramidal neurons. *PLoS One* **5,** e10596
45. Cubelos, B., Briz, C. G., Esteban-Ortega, G. M., and Nieto, M. (2015) Cux1 and Cux2 selectively target basal and apical dendritic compartments of layer II-III cortical neurons. *Dev. Neurobiol.* **75,** 163–172
46. Cubelos, B., and Nieto, M. (2010) Intrinsic programs regulating dendrites and synapses in the upper layer neurons of the cortex. *Commun. Integr. Biol.* **3,** 483–486
47. Blochlinger, K., Bodmer, R., Jack, J., Jan, L. Y., and Jan, Y. N. (1988) Primary structure and expression of a product from cut, a locus involved in specifying sensory organ identity in *Drosophila*. *Nature* **333,** 629–635
48. Neufeld, E. J., Skalnik, D. G., Lievens, P. M., and Orkin, S. H. (1992) Human CCAAT displacement protein is homologous to the *Drosophila* homeoprotein, cut. *Nat. Genet.* **1,** 50–55
49. Quaggin, S. E., Heuvel, G. B., Golden, K., Bodmer, R., and Igarashi, P. (1996) Primary structure, neural-specific expression, and chromosomal localization of Cux-2, a second murine homeobox gene related to *Drosophila* cut. *J. Biol. Chem.* **271,** 22624–22634
50. Harada, R., Bérubé, G., Tamplin, O. J., Denis-Larose, C., and Nepveu, A. (1995) DNA-binding specificity of the cut repeats from the human cut-

like protein. *Mol. Cell. Biol.* **15,** 129–140
51. Harada, R., Dufort, D., Denis-Larose, C., and Nepveu, A. (1994) Conserved cut repeats in the human cut homeodomain protein function as DNA binding domains. *J. Biol. Chem.* **269,** 2062–2067
52. Ramdzan, Z. M., Pal, R., Kaur, S., Leduy, L., Bérubé, G., Davoudi, S., Vadnais, C., and Nepveu, A. (2015) The function of CUX1 in oxidative DNA damage repair is needed to prevent premature senescence of mouse embryo fibroblasts. *Oncotarget* **6,** 3613–3626
53. Ramdzan, Z. M., Vadnais, C., Pal, R., Vandal, G., Cadieux, C., Leduy, L., Davoudi, S., Hulea, L., Yao, L., Karnezis, A. N., Paquet, M., Dankort, D., and Nepveu, A. (2014) RAS transformation requires CUX1-dependent repair of oxidative DNA damage. *PLoS Biol.* **12,** e1001807
54. Luo, J., Emanuele, M. J., Li, D., Creighton, C. J., Schlabach, M. R., Westbrook, T. F., Wong, K. K., and Elledge, S. J. (2009) A genome-wide RNAi screen identifies multiple synthetic lethal interactions with the Ras oncogene. *Cell* **137,** 835–848
55. Luo, J., Solimini, N. L., and Elledge, S. J. (2009) Principles of cancer therapy: oncogene and non-oncogene addiction. *Cell* **136,** 823–837
56. Ramdzan, Z. M., and Nepveu, A. (2014) CUX1, a haploinsufficient tumour suppressor gene overexpressed in advanced cancers. *Nat. Rev. Cancer* **14,** 673–682
57. Ellis, T., Gambardella, L., Horcher, M., Tschanz, S., Capol, J., Bertram, P., Jochum, W., Barrandon, Y., and Busslinger, M. (2001) The transcriptional repressor CDP (Cutl1) is essential for epithelial cell differentiation of the lung and the hair follicle. *Genes Dev.* **15,** 2307–2319
58. Iulianella, A., Vanden Heuvel, G., and Trainor, P. (2003) Dynamic expression of murine Cux2 in craniofacial, limb, urogenital and neuronal primordia. *Gene Expr. Patterns* **3,** 571–577
59. Conforto, T. L., Zhang, Y., Sherman, J., and Waxman, D. J. (2012) Impact of CUX2 on the female mouse liver transcriptome: activation of female-biased genes and repression of male-biased genes. *Mol. Cell. Biol.* **32,** 4611–4627
60. Laz, E. V., Holloway, M. G., Chen, C. S., and Waxman, D. J. (2007) Characterization of three growth hormone-responsive transcription factors preferentially expressed in adult female liver. *Endocrinology* **148,** 3327–3337
61. Yamada, M., Clark, J., McClelland, C., Capaldo, E., Ray, A., and Iulianella, A. (2015) Cux2 activity defines a subpopulation of perinatal neurogenic progenitors in the hippocampus. *Hippocampus* **25,** 253–267
62. Iulianella, A., Sharma, M., Durnin, M., Vanden Heuvel, G. B., and Trainor, P. A. (2008) Cux2 (Cutl2) integrates neural progenitor development with cell-cycle progression during spinal cord neurogenesis. *Development* **135,** 729–741
63. Iulianella, A., Sharma, M., Vanden Heuvel, G. B., and Trainor, P. A. (2009) Cux2 functions downstream of Notch signaling to regulate dorsal interneuron formation in the spinal cord. *Development* **136,** 2329–2334
64. Bachy, I., Franck, M. C., Li, L., Abdo, H., Pattyn, A., and Ernfors, P. (2011) The transcription factor Cux2 marks development of an A-δ sublineage of TrkA sensory neurons. *Dev. Biol.* **360,** 77–86
65. Wittmann, W., Iulianella, A., and Gunhaga, L. (2014) Cux2 acts as a critical regulator for neurogenesis in the olfactory epithelium of vertebrates. *Dev. Biol.* **388,** 35–47
66. Nieto, M., Monuki, E. S., Tang, H., Imitola, J., Haubst, N., Khoury, S. J., Cunningham, J., Gotz, M., and Walsh, C. A. (2004) Expression of Cux-1 and Cux-2 in the subventricular zone and upper layers II-IV of the cerebral cortex. *J. Comp. Neurol.* **479,** 168–180
67. Gingras, H., Cases, O., Krasilnikova, M., Bérubé, G., and Nepveu, A. (2005) Biochemical characterization of the mammalian Cux2 protein. *Gene* **344,** 273–285
68. Hulea, L., and Nepveu, A. (2012) CUX1 transcription factors: from biochemical activities and cell-based assays to mouse models and human diseases. *Gene* **497,** 18–26
69. Sansregret, L., and Nepveu, A. (2008) The multiple roles of CUX1: insights from mouse models and cell-based assays. *Gene* **412,** 84–94
70. Antoine-Bertrand, J., Ghogha, A., Luangrath, V., Bedford, F. K., and Lamarche-Vane, N. (2011) The activation of ezrin-radixin-moesin proteins is regulated by netrin-1 through Src kinase and RhoA/Rho kinase activities and mediates netrin-1-induced axon outgrowth. *Mol. Biol. Cell* **22,** 3734–3746
71. Moon, N. S., Bérubé, G., and Nepveu, A. (2000) CCAAT displacement activity involves Cut repeats 1 and 2, not the Cut homeodomain. *J. Biol. Chem.* **275,** 31325–31334
72. Shen, W. F., Chang, C. P., Rozenfeld, S., Sauvageau, G., Humphries, R. K., Lu, M., Lawrence, H. J., Cleary, M. L., and Largman, C. (1996) Hox homeodomain proteins exhibit selective complex stabilities with Pbx and DNA. *Nucleic Acids Res.* **24,** 898–906
73. Paz-Elizur, T., Elinger, D., Leitner-Dagan, Y., Blumenstein, S., Krupsky, M., Berrebi, A., Schechtman, E., and Livneh, Z. (2007) Development of an enzymatic DNA repair assay for molecular epidemiology studies: distribution of OGG activity in healthy individuals. *DNA Repair* **6,** 45–60
74. Jacobs, A. C., Calkins, M. J., Jadhav, A., Dorjsuren, D., Maloney, D., Simeonov, A., Jaruga, P., Dizdaroglu, M., McCullough, A. K., and Lloyd, R. S. (2013) Inhibition of DNA glycosylases via small molecule purine analogs. *PLoS One* **8,** e81667
75. Moon, N. S., Premdas, P., Truscott, M., Leduy, L., Bérubé, G., and Nepveu, A. (2001) S phase-specific proteolytic cleavage is required to activate stable DNA binding by the CDP/Cut homeodomain protein. *Mol. Cell. Biol.* **21,** 6332–6345
76. Marcotte, R., Brown, K. R., Suarez, F., Sayad, A., Karamboulas, K., Krzyzanowski, P. M., Sircoulomb, F., Medrano, M., Fedyshyn, Y., Koh, J. L., van Dyk, D., Fedyshyn, B., Luhova, M., Brito, G. C., Vizeacoumar, F. J., Vizeacoumar, F. S., Datti, A., Kasimer, D., Buzina, A., Mero, P., Misquitta, C., Normand, J., Haider, M., Ketela, T., Wrana, J. L., Rottapel, R., Neel, B. G., and Moffat, J. (2012) Essential gene profiles in breast, pancreatic, and ovarian cancer cells. *Cancer Discov.* **2,** 172–189
77. Magistretti, P. J., and Pellerin, L. (1996) Cellular bases of brain energy metabolism and their relevance to functional brain imaging: evidence for a prominent role of astrocytes. *Cerebral Cortex* **6,** 50–61
78. Bruckner, B. A., Ammini, C. V., Otal, M. P., Raizada, M. K., and Stacpoole, P. W. (1999) Regulation of brain glucose transporters by glucose and oxygen deprivation. *Metabolism* **48,** 422–431
79. Nouspikel, T., and Hanawalt, P. C. (2000) Terminally differentiated human neurons repair transcribed genes but display attenuated global DNA repair and modulation of repair Gene expression. *Mol. Cell. Biol.* **20,** 1562–1570
80. Viswanathan, A., You, H. J., and Doetsch, P. W. (1999) Phenotypic change caused by transcriptional bypass of uracil in nondividing cells. *Science* **284,** 159–162
81. Vadnais, C., Davoudi, S., Afshin, M., Harada, R., Dudley, R., Clermont, P. L., Drobetsky, E., and Nepveu, A. (2012) CUX1 transcription factor is required for optimal ATM/ATR-mediated responses to DNA damage. *Nucleic Acids Res.* **40,** 4483–4495
82. Hill, J. W., and Evans, M. K. (2006) Dimerization and opposite base-dependent catalytic impairment of polymorphic S326C OGG1 glycosylase. *Nucleic Acids Res.* **34,** 1620–1632
83. Crenshaw, C. M., Nam, K., Oo, K., Kutchukian, P. S., Bowman, B. R., Karplus, M., and Verdine, G. L. (2012) Enforced presentation of an extrahelical guanine to the lesion recognition pocket of human 8-oxoguanine glycosylase, hOGG1. *J. Biol. Chem.* **287,** 24916–24928
84. Banerjee, A., Yang, W., Karplus, M., and Verdine, G. L. (2005) Structure of a repair enzyme interrogating undamaged DNA elucidates recognition of damaged DNA. *Nature* **434,** 612–618
85. Bjørås, M., Seeberg, E., Luna, L., Pearl, L. H., and Barrett, T. E. (2002) Reciprocal flipping underlies substrate recognition and catalytic activation by the human 8-oxo-guanine DNA glycosylase. *J. Mol. Biol.* **317,** 171–177
86. Bruner, S. D., Norman, D. P., and Verdine, G. L. (2000) Structural basis for recognition and repair of the endogenous mutagen 8-oxoguanine in DNA. *Nature* **403,** 859–866
87. David, S. S., O'Shea, V. L., and Kundu, S. (2007) Base-excision repair of oxidative DNA damage. *Nature* **447,** 941–950
88. Chen, L., Haushalter, K. A., Lieber, C. M., and Verdine, G. L. (2002) Direct visualization of a DNA glycosylase searching for damage. *Chem. Biol.* **9,** 345–350
89. Moffat, J., Grueneberg, D. A., Yang, X., Kim, S. Y., Kloepfer, A. M., Hinkle, G., Piqani, B., Eisenhaure, T. M., Luo, B., Grenier, J. K., Carpenter, A. E., Foo, S. Y., Stewart, S. A., Stockwell, B. R., Hacohen, N., Hahn, W. C., Lander, E. S., Sabatini, D. M., and Root, D. E. (2006) A lentiviral RNAi library for human and mouse genes applied to an arrayed viral high-content screen. *Cell* **124,** 1283–1298